

Article

Study on Synergistic Strengthening of Gold Extraction with Copper Ethylenediamine Thiosulfate Using Pyrite and Nickel Ions

Xuecong Qin ¹, Tao Zhang ^{1,*}, Futing Zi ², Hongbo Zhang ^{1,*} and Guoping Li ¹

¹ School of Resource and Environmental Engineering, Inner Mongolia University of Technology, Hohhot 010020, China; xuecong1319@imut.edu.cn (X.Q.); liguoping@imut.edu.cn (G.L.)

² Faculty of Science, Kunming University of Science and Technology, Kunming 650500, China; 20030068@kust.edu.cn

* Correspondence: zhangtao@imut.edu.cn (T.Z.); zhanghongbo@imut.edu.cn (H.Z.); Tel.: +86-152-4808-2273 (T.Z.)

Abstract: Gold leaching using the copper–ethylenediamine–thiosulfate (Cu^{2+} -en- $\text{S}_2\text{O}_3^{2-}$) system, which contains copper–ethylenediamine complexes, instead of the use of copper–ammonia catalysis, is environmentally friendly and cost-effective. In this study, pyrite and Ni^{2+} were added to the Cu^{2+} -en- $\text{S}_2\text{O}_3^{2-}$ system to clarify their individual and combined influence on gold leaching. The result obtained showed that when pyrite and Ni^{2+} were separately added to the system, the dissolution of gold was significantly inhibited. However, the disappearance of the negative impacts of these two substances when they were simultaneously added to the system revealed that they exhibited a synergistic effect on gold dissolution. Notably, Ni^{2+} weakened the promotional effect of pyrite on the formation of a Cu-containing passivation layer on the gold surface. Furthermore, the separate addition of Ni^{2+} and pyrite increased the corrosion potential of gold; thus, gold dissolution was inhibited. However, when added together, they brought about a decrease in the corrosion potential of gold, while increasing its dissolution rate. These findings provide a reference for the efficient extraction of pyrite-associated gold, which can be applied to improve the green extraction process of gold.

Keywords: pyrite; nickel ion; gold extraction; thiosulphate; ethylenediamine



Citation: Qin, X.; Zhang, T.; Zi, F.; Zhang, H.; Li, G. Study on Synergistic Strengthening of Gold Extraction with Copper Ethylenediamine Thiosulfate Using Pyrite and Nickel Ions. *Minerals* **2024**, *14*, 2. <https://doi.org/10.3390/min14010002>

Academic Editors: Jiajia Wu, Jaeheon Lee and Kenneth N. Han

Received: 9 October 2023

Revised: 12 December 2023

Accepted: 14 December 2023

Published: 19 December 2023



Copyright: © 2023 by the authors. Licensee MDPI, Basel, Switzerland. This article is an open access article distributed under the terms and conditions of the Creative Commons Attribution (CC BY) license (<https://creativecommons.org/licenses/by/4.0/>).

1. Introduction

Currently, due to process simplicity and cost efficiency, gold is primarily extracted using the cyanide method. However, this method generates large amounts of hazardous wastes and poses a serious health risk to humans [1]. In the past few decades, the traditional Cu^{2+} - NH_3 - $\text{S}_2\text{O}_3^{2-}$ gold-leaching method has been investigated as one of the most promising alternatives to cyanidation. This method involves the use of Cu(II) as a catalyst to leach gold from its ore [2–4], and it offers several advantages, such as non-toxicity, high efficiency, low cost (the price per ton is cheaper than that associated with the cyanide method), strong adaptability to the ore, and decreased equipment corrosion. Additionally, it is also suitable for the leaching of several carbonaceous gold ores as well as complex gold sulphide ores [5,6]. Therefore, since its advent, its industrial application as a gold extraction method has been extensively studied.

The minerals that are associated with gold ores can affect thiosulphate stability as well as gold-leaching behaviour [7,8]. Usually, gold is symbiotic or is associated with sulphide minerals, especially pyrite (FeS_2) [9], which influences its leaching in thiosulphate solution by accelerating the decomposition of thiosulphate and partially dissolving in the ammonia–thiosulphate solution [5]. Therefore, strategies aimed at mitigating the harmful effects of pyrite are essential for the realization of the thiosulphate leaching of gold. In recent years, many studies have been focused on the use of various additives to reduce reagent consumption and enhance gold extraction from sulphide minerals [10,11].

In addition to being influenced by Au-containing sulphide ores as well as associated ores, the dissolution of metal ions in the thiosulphate system can also be promoted or hindered by a variety of metal impurities, given that these metal impurities can consume thiosulphate or bring about changes in the reaction on the gold surface and affect the recovery of gold from the leaching solution [12–14]. Additionally, Arima [15] and Xu [16] observed that the use of Ni instead of Cu as a catalyst can reduce the consumption of thiosulphate and accelerate gold ore leaching. Notably, the effect of metal ions on gold dissolution depends on the ionic species of the metals as well as their concentrations, the chemical properties of the solution, and the reaction that takes place on the gold surface.

In the early stage of our research, to form the Cu^{2+} -en- $\text{S}_2\text{O}_3^{2-}$ gold-leaching system, we proposed the use of ethylenediamine as an alternative to ammonia in the conventional Cu^{2+} - NH_3 - $\text{S}_2\text{O}_3^{2-}$ system and conducted a series of related experimental studies [17,18]. The Cu^{2+} -en- $\text{S}_2\text{O}_3^{2-}$ system was found to favour the dissolution of gold and the reduction of thiosulphate consumption to a greater extent, and it showed applicability to fine-grained coated carbonaceous gold ores. However, the effect of sulphide minerals containing different metals on this leaching system remains unclear.

Herein, we investigated the individual and synergistic effects of pyrite and Ni^{2+} on gold leaching in the Cu^{2+} -en- $\text{S}_2\text{O}_3^{2-}$ system. These findings have guiding significance and can serve as a reference for the promotion of the commercial application of the non-cyanide extraction of gold from pyrite-associated ores.

2. Experimental Setup

2.1. Minerals, Reagents, and Characterisation

The pure pyrite samples used in this study were purchased from the Chinese Museum. The pure pyrite was crushed and ground to 100% passing through a 75 μm sieve and stored in a nitrogen-filled airtight plastic bag to prevent further oxidation [7]. Furthermore, the surface area of the gold foil (purity, 99.99%; thickness, 0.1 mm) [8] that was used in the leaching experiments in this study was 1.0 cm^2 . Analytically pure copper sulfate pentahydrate, sodium thiosulfate, ethylenediamine, hydrogen peroxide (30% *w/v*), sodium chloride, and hydrochloric acid were used in the experiments. Metal stock solutions of nickel were made in deionised water with $\text{NiCl}_2 \cdot 6\text{H}_2\text{O}$ (chemical grade). For all the reagents used to prepare solutions of desired concentrations in all the experiments in this study, deionised water was used.

2.2. Experimental, Analytical, and Electrochemical Procedures

Experiments were performed in a 250 mL volumetric flask using a stirrer at a rotating speed of 250 rpm. The gold foil (99.99% Au) surfaces were polished by 2000-grid sandpaper, washed with acetone twice, and rinsed 8 times with deionised water before each test. The gold foil was suspended in the upper part of the leaching reactor with a nylon thread, ensuring no contact with the volumetric flask wall during leaching. The leaching system was a mixture of 0.1 mol/L $\text{Na}_2\text{S}_2\text{O}_3$, 0.005 mol/L CuSO_4 , and 0.01 mol/L en (conditions: pH = 10, temperature = 25 °C). The specific leaching experimental methods used in this study were as previously described [17]. Detailed descriptions of the analysis methods for the determination of the concentration of gold in the prepared solutions have been described in a previous study [17]. Thiosulfate concentration was analysed via iodometry [18]. All of the experimental procedures and sample analysis procedures in this article are detailed in the Supplementary Material at the end of this article.

A PHI5000 Versa Probe II (ULVAC-PHI, Japan, Binzhou Chuangyuan equipment machinery manufacturing Co., Ltd. agent) with an Al $K\alpha$ X-ray source was used to identify the elemental composition of the leached gold foil samples as well as that of the pyrite surface. Thus, Cu 2p, Fe 2p, and S 2p spectra were obtained. To determine the atomic ratio of the sample under analysis, each spectrum was then fitted and analysed using Multi Pak Spectrum software version 2.1. The C 1s spectrum of 284.8 eV was used as a calibration spectrum for binding energy. The Pro X model scanning electron microscope (Phenom,

Rotterdam, The Netherlands) was used to observe the surface micro-morphology of the leached gold foils as well as that of the pyrite samples.

To perform the electrochemical test, a three-electrode system, with gold foil (15 mm × 15 mm × 0.1 mm) as the working electrode, platinum foil (10 mm × 10 mm × 0.2 mm) as the counter electrode, and the saturated calomel electrode (SCE) as the reference electrode, was used. All the electrochemical measurements were performed on a CHI600E workstation at room temperature. Before implementing the electrochemical method, the open-circuit potential (E_{ocp}) of the Cu^{2+} -en- $S_2O_3^{2-}$ gold-leaching system (0.1 M $Na_2S_2O_3$ + 0.005 M $CuSO_4$ + 0.01 M en) was measured so as to ensure the stability of the system during the electrochemical measurement. The open circuit voltage of the system was -0.04 V, and during the experiment, a mixed solution of 0.1 M Na_2SO_3 and 5 mM $[Cu(en)_2]^{2+}$ was used as the electrolyte, and a solution of Ni^{2+} (8 mg/L) or 1 g of pure pyrite was added to the system. The Tafel curve corresponding to the system was obtained at a scan rate of 1 mV/s in the open circuit potential (OCP) within the voltage range of -0.04 ± 0.5 V/SCE.

3. Results and Discussion

3.1. Mineral Characterisation

The mineralogical composition of the pyrite samples was analysed via X-ray fluorescence spectroscopy (XRF). The analysis results are shown in Table 1.

Table 1. Chemical composition of pyrite (%).

| Component | FeS ₂ | SiO ₂ | As ₂ O ₃ |
|-----------|------------------|------------------|--------------------------------|
| % (w/w) | 98.6 | 0.86 | 0.54 |

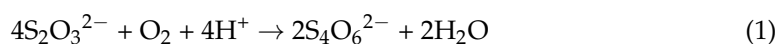
3.2. Effects of Pyrite on Gold Leaching in the Cu^{2+} -en- $S_2O_3^{2-}$ System

3.2.1. Effects of Pyrite on Gold Dissolution and Thiosulphate Decomposition

When mineral particles are added to the leaching system, the mutual friction between gold foil and minerals will also enhance the dissolution of gold leaf in the system during the continuous stirring process. In this case, it is not possible to determine whether the final result is determined by the effect of friction on gold dissolution or the effect of pyrite on gold dissolution. Therefore, in order to eliminate the effect of continuous friction between mineral particles and gold foil on gold dissolution in the system, only the specific influence of pyrite on gold dissolution is determined. An amount of 1g quartz was selected as the control group for the adding pyrite [7,19–21].

The effects of pyrite on gold foil dissolution and thiosulphate consumption in the Cu^{2+} -en- $S_2O_3^{2-}$ system were investigated using quartz as the blank control. Typically, 1 g of pyrite or 1 g of quartz was added to the leaching system, and samples were taken at pre-defined intervals for the analysis of the gold content of the leaching solution (Figure 1). In the case of quartz, the amount of dissolved gold increased with time in an approximately linear manner, whereas pyrite strongly inhibited gold dissolution.

The presence of pyrite brought about a significant increase in thiosulphate consumption within 34 h of leaching (Figure 2). However, in the presence of quartz, only 14.6% of thiosulphate was degraded within 34 h of leaching, indicating that this mineral has no significant effect on thiosulphate decomposition. This observation is consistent with the known chemical inertness of quartz in ammonia–thiosulphate solutions [22]. Specifically, when pyrite was added to the leaching solution, there was a sharp increase in thiosulphate consumption, which reached 36.52% after 34 h of leaching. This is significantly higher than that observed in the presence of quartz. This implies that pyrite significantly accelerated thiosulphate decomposition [5]. Some researchers think that because of its semiconducting properties, pyrite can be used as a conductive band for electron transfer between thiosulphate and oxygen, with the related reaction given by XU and SCHOONEN [23].



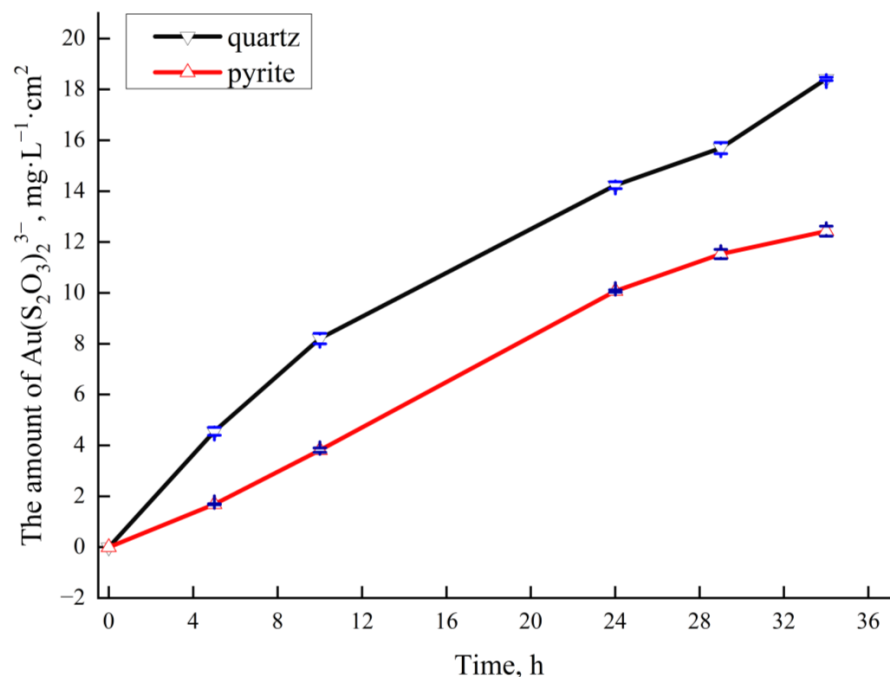


Figure 1. Variation of the amount $\text{Au}(\text{S}_2\text{O}_3)_2^{3-}$ with time during gold leaching using the Cu^{2+} -en- $\text{S}_2\text{O}_3^{2-}$ system in the presence of pyrite and quartz (mineral content: pyrite, 1 g; quartz, 1 g).

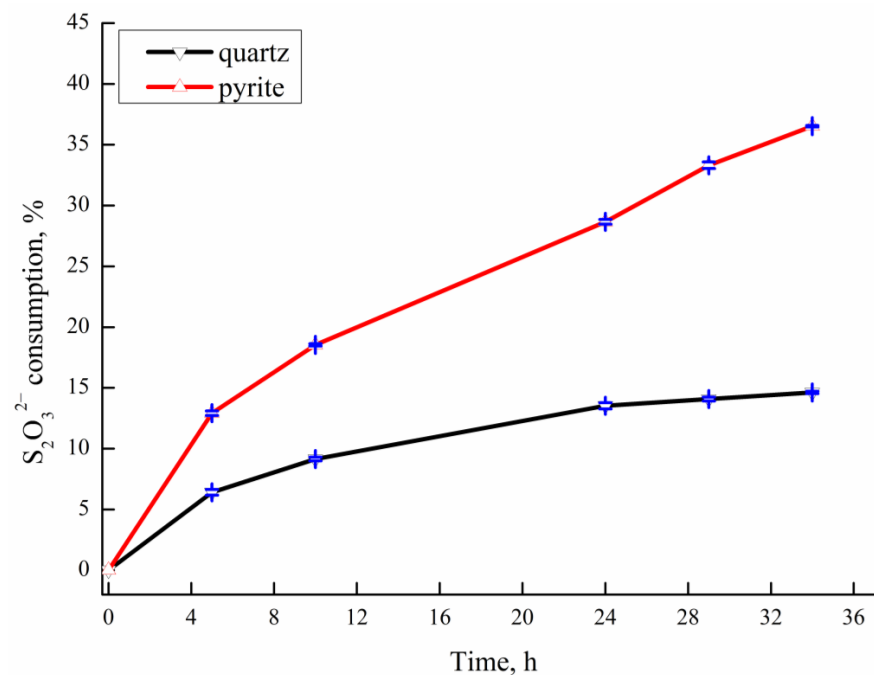


Figure 2. Variation of thiosulfate consumption with time during gold leaching using the Cu^{2+} -en- $\text{S}_2\text{O}_3^{2-}$ system in the presence of pyrite and quartz (mineral content: pyrite, 1 g; quartz 1 g).

However, the rate of thiosulphate consumption in the leaching solution decreased with increasing leaching time. This observation was attributed to the oxidation of pyrite by $\text{Cu}(\text{I}/\text{II})$ species during leaching to form $\text{S}_2\text{O}_3^{2-}$, bringing about an increase in the thiosulphate content of the leaching solution [23,24].

In the presence of $\text{Cu}(\text{II})$ ions, thiosulphate can be oxidised to tetrathionate and trithionate [25], of which trithionate can be further decomposed to release thiosulphate and sulphite. Additionally, polythionate can reduce $\text{Cu}(\text{II})$ ions, thus, bringing about a decrease in the rate of gold leaching [26]; this accounts for the inhibitory effect of pyrite on

gold dissolution. Additionally, thiosulphate decomposition can induce the formation of a passivation layer consisting of elemental S and copper sulphide, which prevents the thiosulphate solution from diffusing to the gold surface [27–29]. Thus, the increased thiosulphate consumption in the presence of pyrite may result in a greater degree of passivation.

3.2.2. Effects of Ni^{2+} on Gold Dissolution and Thiosulphate Decomposition

Figure 3 shows the effect of different Ni^{2+} concentrations on the dissolution of gold in the Cu^{2+} -en- $\text{S}_2\text{O}_3^{2-}$ system. It can be seen from the figure that when the nickel ion concentration is 8 mg/L, the gold concentration after 34 h is 5.85 mg/L, and when the $[\text{Ni}^{2+}]$ increases, the amount of gold dissolved will be further reduced. The gold concentration in the blank control group (i.e., 0 mg/L Ni^{2+}) was 8.59 mg/L. Therefore, it is determined that different concentrations of Ni^{2+} can inhibit the dissolution of gold, and as $[\text{Ni}^{2+}]$ increases, the inhibitory effect becomes stronger. Because Ni^{2+} freely competed with Cu^{2+} , it reduced the concentration of $[\text{Cu}(\text{en})_2]^{2+}$ and brought about a decrease in the amount of gold dissolution. Conversely, a further increase in the concentration of Ni^{2+} significantly promoted the formation of NiS [8]. Therefore, the presence of nickel ions only in the Cu^{2+} -en- $\text{S}_2\text{O}_3^{2-}$ system passivates the gold surface during leaching.

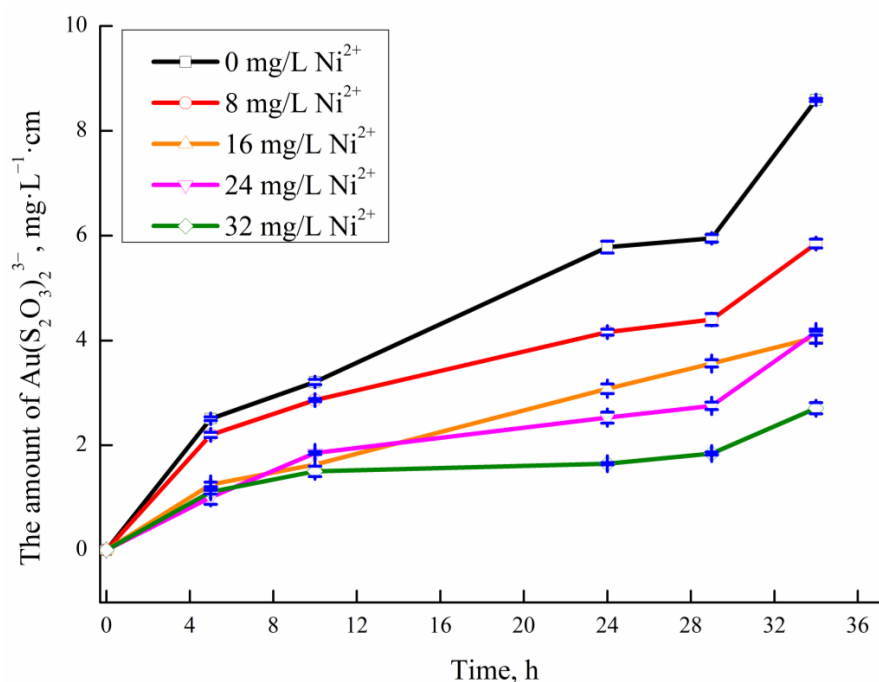


Figure 3. Variation of amount $\text{Au}(\text{S}_2\text{O}_3)_2^{3-}$ with time during gold leaching using the Cu^{2+} -en- $\text{S}_2\text{O}_3^{2-}$ system in the presence of Ni^{2+} .

Figure 4 shows that under standard conditions ($[\text{S}_2\text{O}_3^{2-}] = 0.1 \text{ mol/L}$, $[\text{Cu}^{2+}] = 0.005 \text{ mol/L}$, $[\text{en}] = 0.01 \text{ mol/L}$), thiosulphate consumption increased with increasing $[\text{Ni}^{2+}]$. This observation could be attributed to the ability of these metal ions to complex thiosulphate [12].

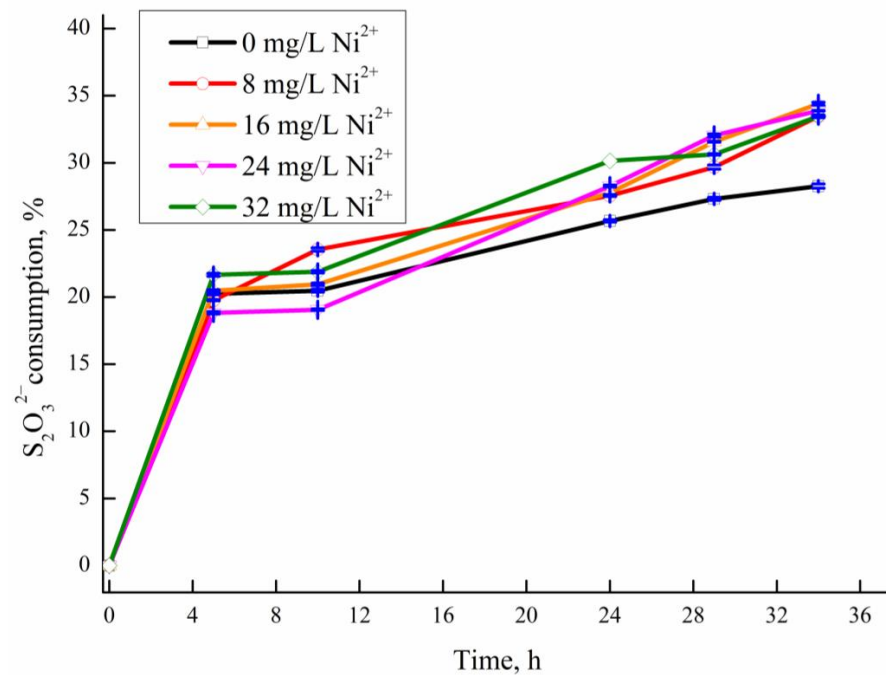


Figure 4. Variation of thiosulfate consumption with time during gold leaching using the Cu^{2+} -en- $\text{S}_2\text{O}_3^{2-}$ in the presence of Ni^{2+} .

3.3. Effects of Ni^{2+} and Pyrite on Thiosulphate Decomposition and Gold Dissolution

Figure 5 illustrates that in the presence of pyrite, thiosulphate consumption increased with increasing $[\text{Ni}^{2+}]$. In addition, as $[\text{Ni}^{2+}]$ increased from 0 to 8 mg/L, thiosulphate consumption increased from 36.52 to ~40.17%. Furthermore, when $[\text{Ni}^{2+}]$ exceeded 24 mg/L, the rate of thiosulfate consumption was greater, and in the presence of a higher dose of Ni^{2+} (24 mg/L), the rate of thiosulfate consumption further increased to ~43.84%, which is ~7.32% higher than that observed in pyrite systems without Ni^{2+} .

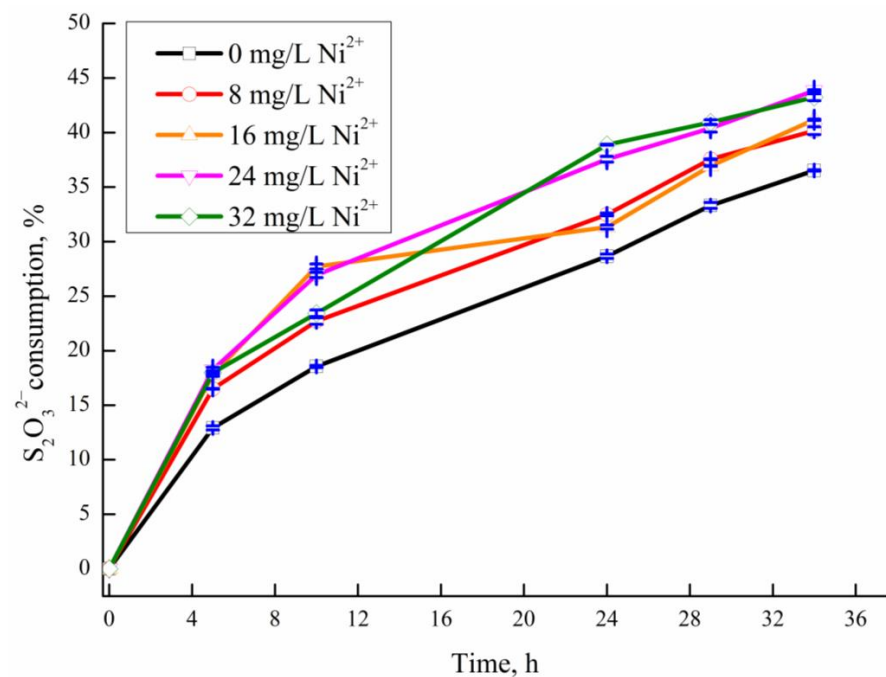


Figure 5. Variation of the thiosulfate consumption with time during gold leaching using the Cu^{2+} -en- $\text{S}_2\text{O}_3^{2-}$ system under different Ni^{2+} concentrations and 1 g of pyrite.

The increased thiosulphate consumption observed in the presence of Ni^{2+} and pyrite is possibly due to the promotional effect of Ni^{2+} ions adsorbed on pyrite on thiosulphate decomposition as well as their strongly thiophilic nature, which allows them to be complexed by thiosulphate; hence, the consumption of large amounts of sodium thiosulfate. In addition, when adsorbed onto the surface of pyrite (especially at high-energy defect sites and grain boundaries), the above cations may partly replace Fe^{2+} . This results in the combination of Fe^{2+} and oxygen, which accelerates pyrite surface oxidation and increases thiosulphate consumption. Moreover, the adsorption of Ni^{2+} may also change the semiconductor properties of the surface of pyrite. Therefore, the addition of Ni^{2+} and pyrite can bring about a sharp increase in thiosulphate consumption.

Figure 6 shows the effect of $[\text{Ni}^{2+}]$ on the concentration of gold during leaching using the Cu^{2+} -en- $\text{S}_2\text{O}_3^{2-}$ system in the presence of pyrite. This figure reveals that an increase in $[\text{Ni}^{2+}]$ resulted in a significant increase in Au solubility, and the range of $[\text{Ni}^{2+}]$ that was most favourable for gold dissolution was 8–24 mg/L. Furthermore, as $[\text{Ni}^{2+}]$ increased from 0 to 8 mg/L, the amount of gold dissolution increased from 12.43 to 22.01 mg/L·cm², i.e., to a value much higher than that observed in the quartz slurry without Ni^{2+} (12.5 mg/L·cm², Figure 1). Even though Au solubility was lower than 22.01 mg/L·cm² at $[\text{Ni}^{2+}] = 24$ and 32 mg/L, it was still above the value obtained in the presence of pyrite only. Therefore, the presence of pyrite in the leaching system alongside small amounts of Ni^{2+} enhanced gold dissolution.

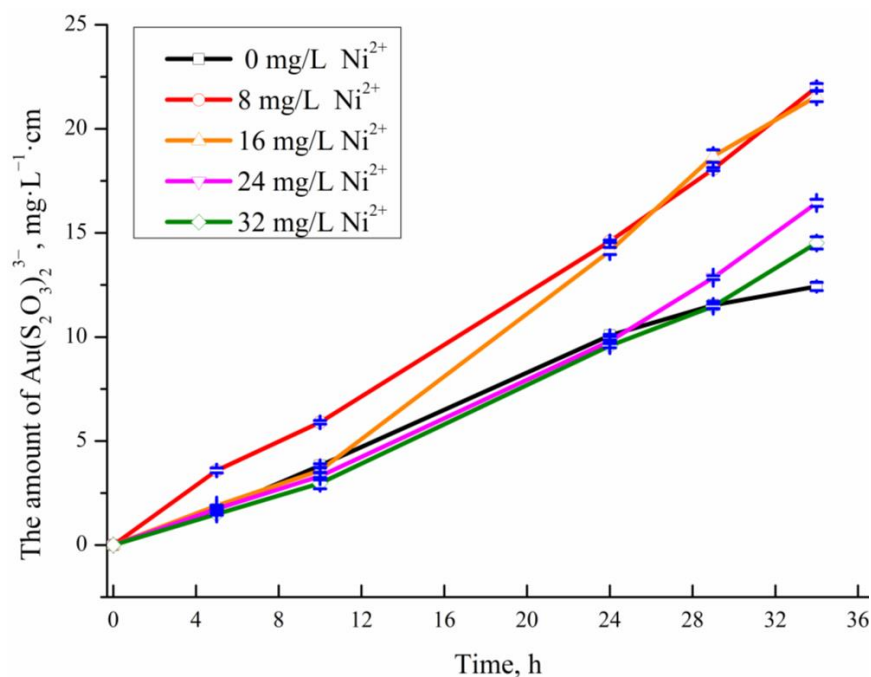


Figure 6. Variation of gold dissolution with time during gold leaching using the Cu^{2+} -en- $\text{S}_2\text{O}_3^{2-}$ system under different $[\text{Ni}^{2+}]$ and 1 g of pyrite.

3.4. Scanning Electron Microscopy (SEM) Imaging

3.4.1. SEM Imaging of Leached Gold Foil

To study the effects of Ni^{2+} and pyrite on the leaching of gold using the Cu^{2+} -en- $\text{S}_2\text{O}_3^{2-}$ system, the morphologies of pyrite and gold foil after leaching were probed via SEM (Figure 7). Thus, it was observed that the surface of the gold foil that was leached in the presence of both additives (Ni^{2+} and pyrite) showed a different morphology and corrosion degree compared with those leached in the presence of pyrite only.

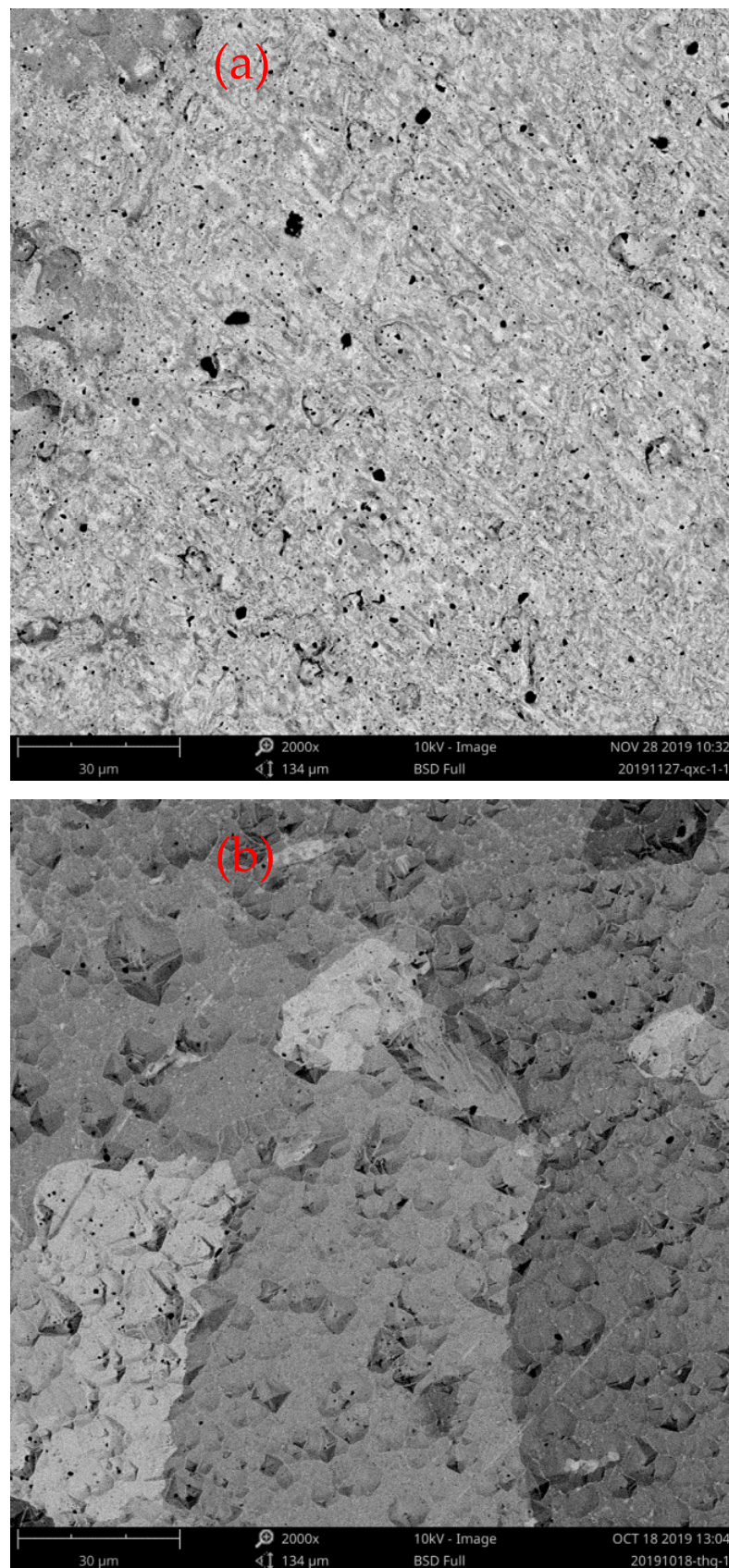


Figure 7. Scanning electron microscopy (SEM) images of gold foils after leaching for 34 h. (a) SEM image of gold foil leached using the Cu^{2+} -en- $\text{S}_2\text{O}_3^{2-}$ system in the presence of Ni^{2+} and pyrite; (b) SEM image of gold foil leached using the Cu^{2+} -en- $\text{S}_2\text{O}_3^{2-}$ system in the presence of pyrite only.

The surface of the gold foil leached in the presence of Ni^{2+} (8 mg/L) and 1 g of pyrite showed numerous black spots (Figure 7a) as well as scarring features, such as rough pitting, which resulted in the easy corrosion of the gold surface around the affected areas. Additionally, some adsorbed particles were also observed on the gold foil surface. In the presence of pyrite only, the leached gold foil showed only minimal signs of corrosion with no obvious corrosion traces (Figure 7b). However, a thick passivation film was formed on the surface of the gold foil, preventing it from contacting the leaching liquid. This finding supported the hypothesis that gold leaching is severely hindered in the presence of pyrite. According to Feng and van Deventer, colloidal metal particles formed during leaching adhere to the surface of gold, deactivating it and preventing its dissolution [12].

3.4.2. SEM Imaging of Leached Pyrite Surface

Figure 8a shows that numerous fine particles were adsorbed onto the surface of pyrite after leaching in the presence of Ni^{2+} (8 mg/L) and 1 g of pyrite. Additionally, several small pyrite particles were agglomerated, and this reduced the contact area between pyrite and the leaching solution, hindering the formation of a Cu-containing passivation layer on the surface of the gold foil, and facilitating gold dissolution. Figure 8b shows that the pyrite that was added to the leaching system in the absence of Ni^{2+} had a light, smooth, and compact surface, without the agglomeration of fine particles.

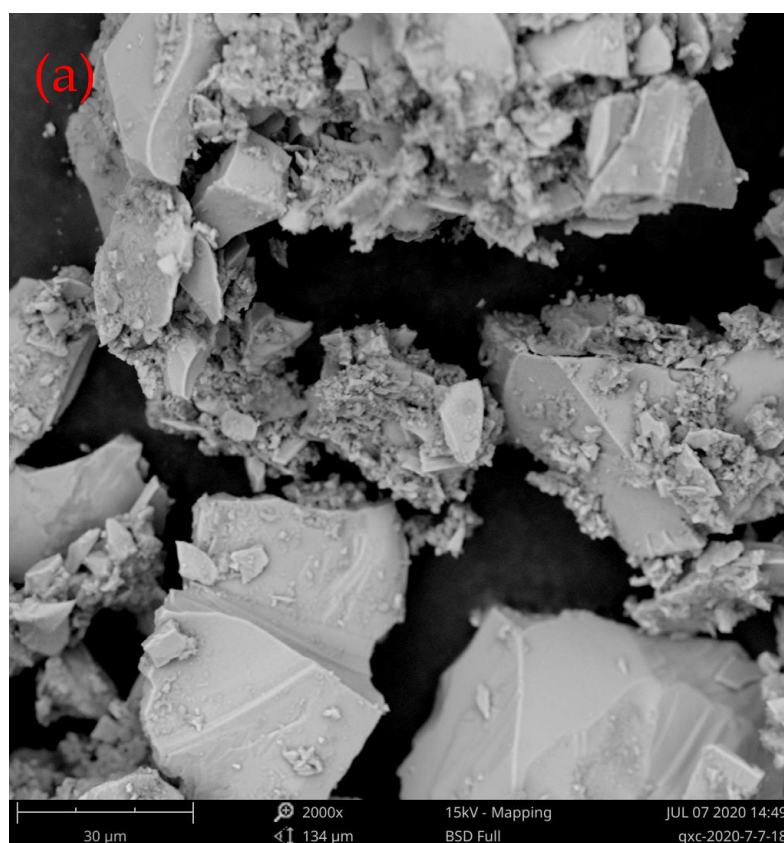


Figure 8. Cont.

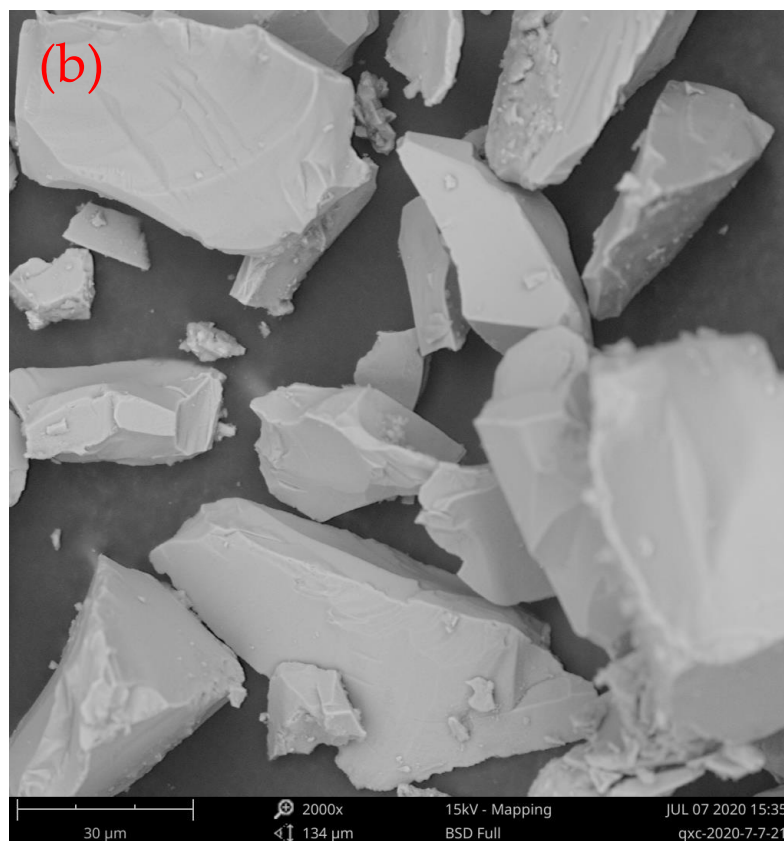


Figure 8. Scanning electron microscopy (SEM) images of pyrite samples after leaching for 34 h. (a) SEM image of pyrite leached using the Cu^{2+} -en- $\text{S}_2\text{O}_3^{2-}$ system in the presence of Ni^{2+} and pyrite; (b) SEM image of pyrite leached using the Cu^{2+} -en- $\text{S}_2\text{O}_3^{2-}$ leaching system in the presence of pyrite only.

3.5. XPS Analysis

3.5.1. XPS Analysis of Gold Surface after Leaching

The Cu 2p, S 2p, and Fe 2p spectra of the gold surface are shown in Figures 9a,b–11a,b. Notably, hardly any nickel was present on the surfaces of the gold foil and pyrite after leaching in the presence of both pyrite and Ni^{2+} . Table 2 shows the surface elemental contents of the gold foil leached in the presence of both Ni^{2+} and pyrite, while Table 3 shows the elemental contents obtained when the gold foil was leached in the presence of pyrite only.

Table 2. Atomic concentration of gold leached using the Cu^{2+} -en- $\text{S}_2\text{O}_3^{2-}$ leaching system in the presence of Ni^{2+} (8 mg/L) and pyrite (1 g).

| Element | O | S | Fe | Ni | Cu | Au |
|-------------------|------|------|------|----|------|------|
| Concentration (%) | 22.9 | 17.4 | 3.00 | 0 | 0.50 | 56.2 |

Table 3. Atomic concentration of gold leached using the Cu^{2+} -en- $\text{S}_2\text{O}_3^{2-}$ leaching system in the presence of pyrite (1 g) only.

| Element | O | S | Fe | Cu | Au |
|-------------------|------|------|------|------|------|
| Concentration (%) | 19.8 | 12.1 | 2.97 | 8.48 | 56.7 |

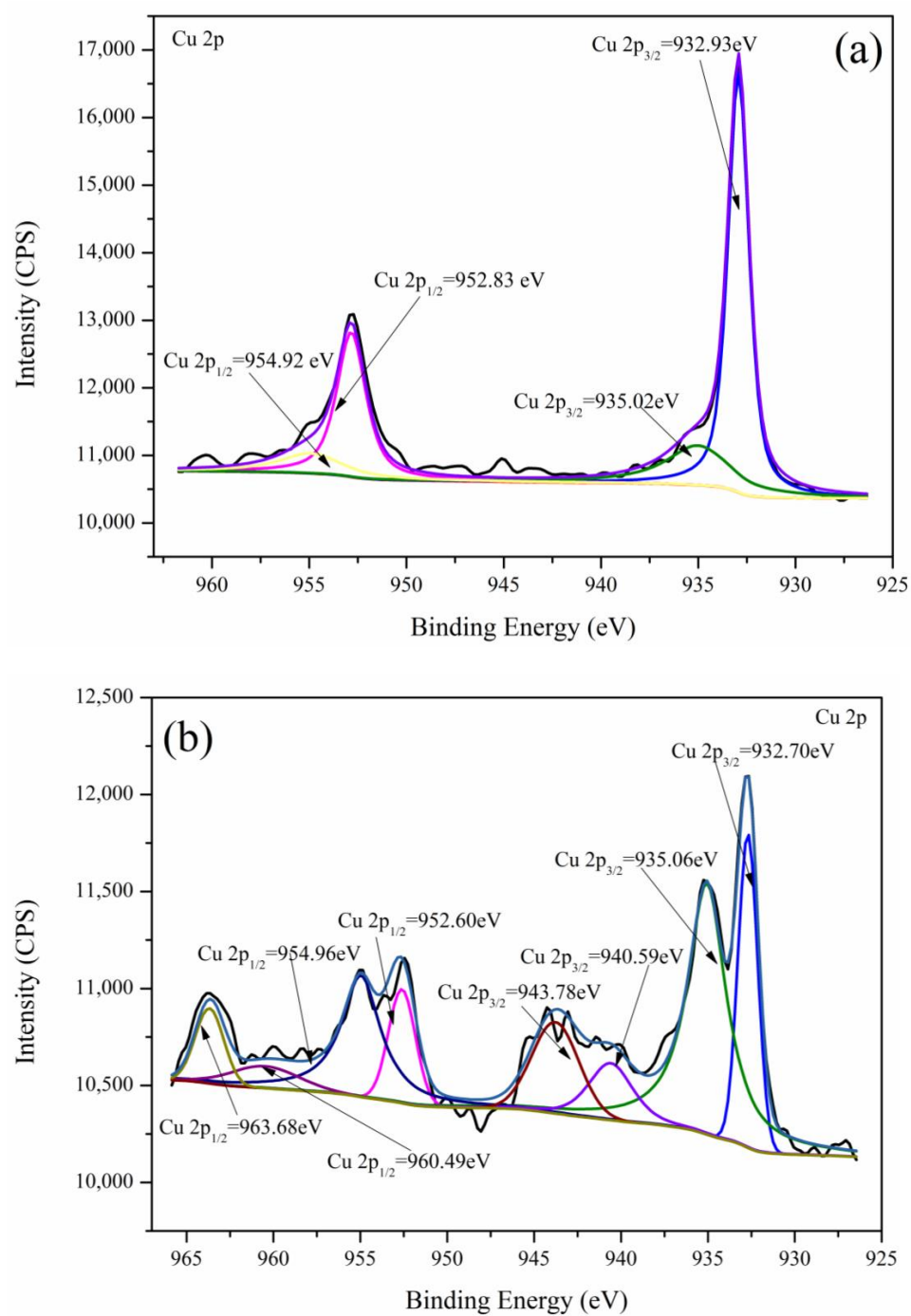


Figure 9. Cu 2p XPS spectra of gold foil surface after leaching in the presence of pyrite; (a) with the addition of Ni^{2+} and (b) without the addition of Ni^{2+} .

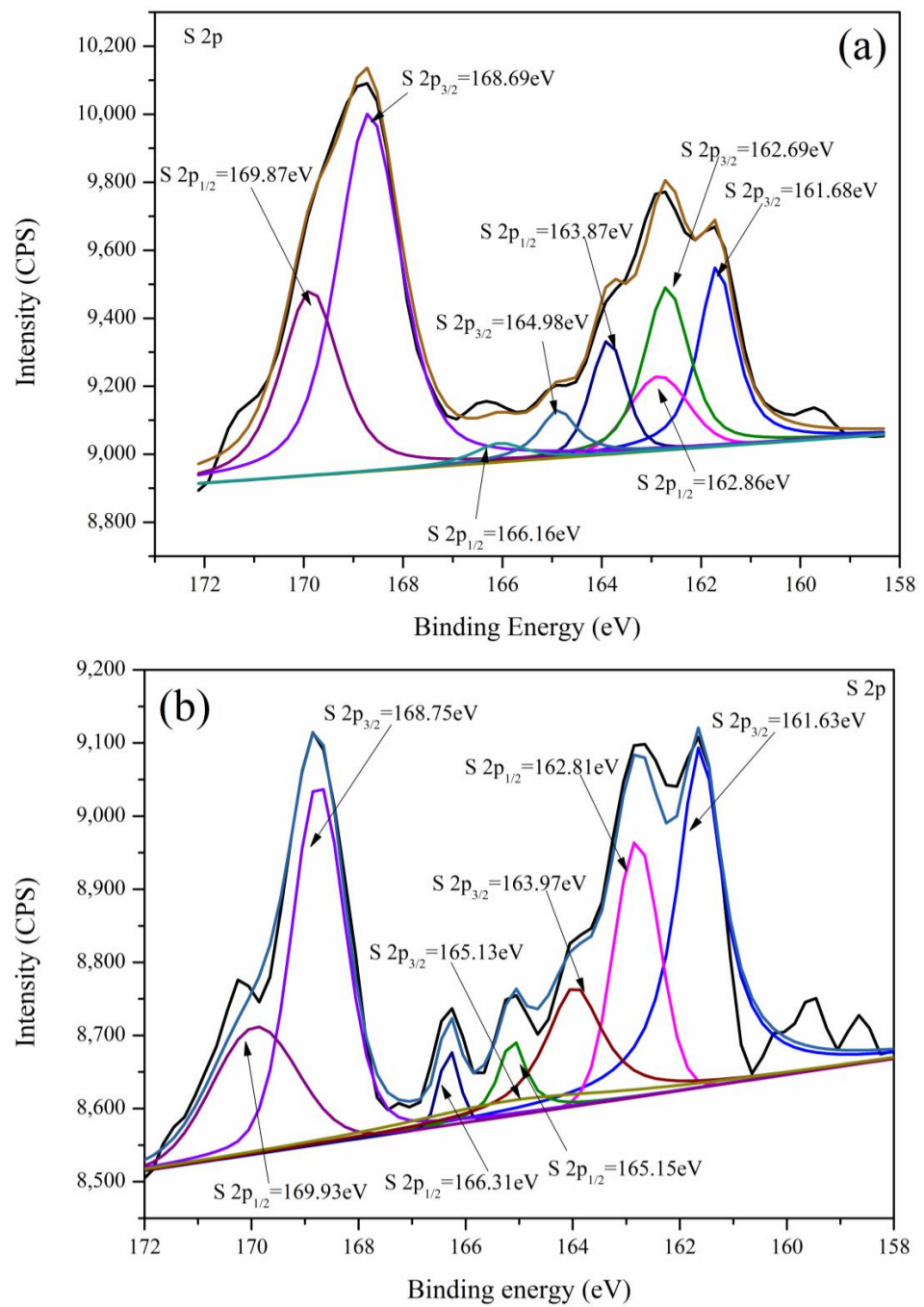


Figure 10. S 2p XPS spectra of gold foil surface after leaching in the presence of pyrite (g). (a) With the addition of Ni²⁺ and (b) without the addition of Ni²⁺.

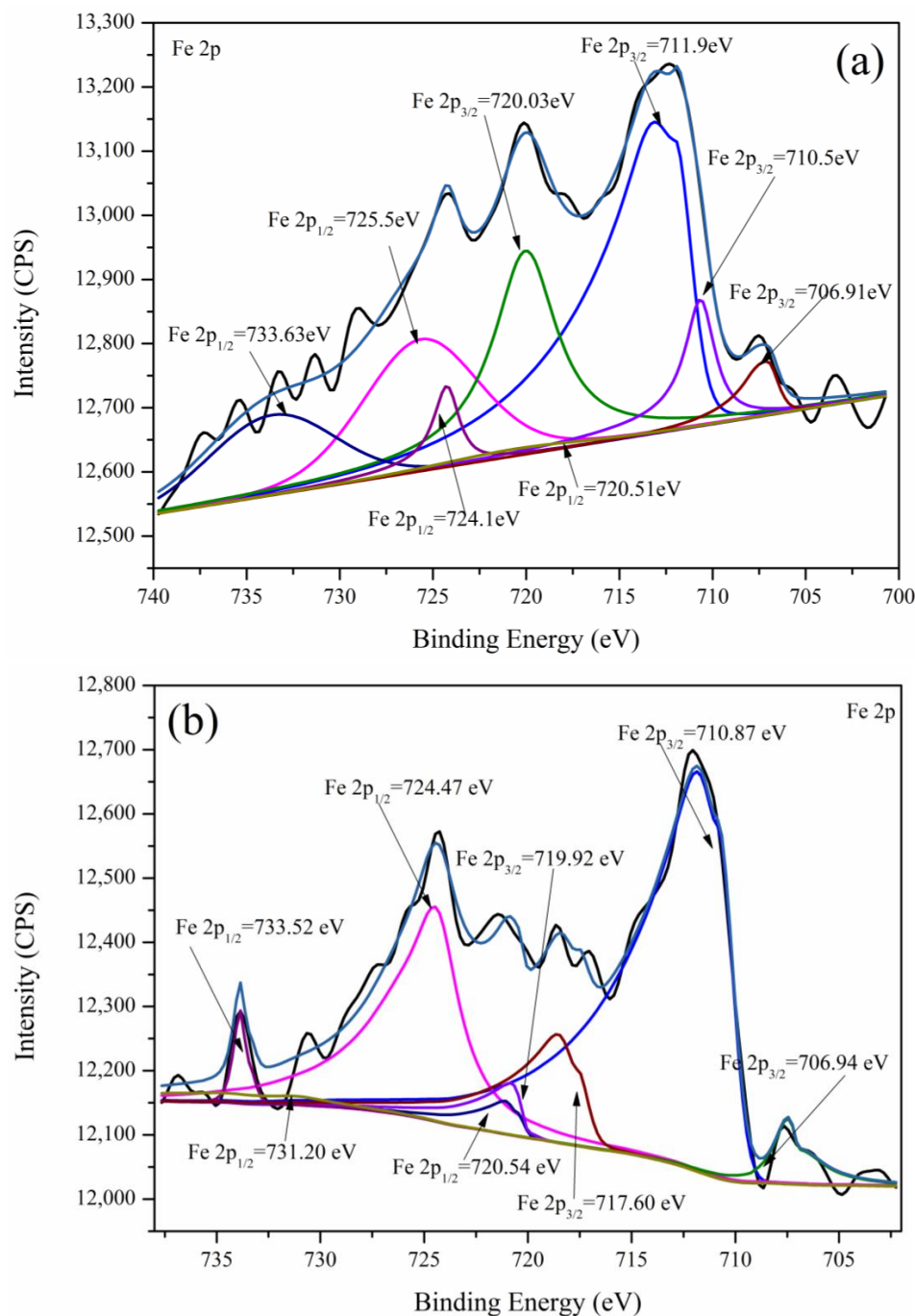


Figure 11. Fe 2p XPS spectra of gold surfaces after leaching in the presence of pyrite (1 g). (a) With the addition of Ni²⁺ and (b) without the addition of Ni²⁺.

Figure 9a,b and Tables 4 and 5 show the Cu 2p spectra of the surface of the gold foil that was leached in the Cu²⁺-en-S₂O₃²⁻ system containing pyrite with and without Ni²⁺, respectively, which were mainly Cu₂S [30] and CuS/Cu(OH)₂, respectively [31,32]. By comparing Tables 2 and 3, it is found that the copper element content on the surface of the gold foil after leaching in the system containing Ni²⁺ and pyrite is much smaller than that when only pyrite is leached. Therefore, Ni²⁺ is likely to weaken the promoting effect of pyrite on the deposition of copper on the gold surface [5].

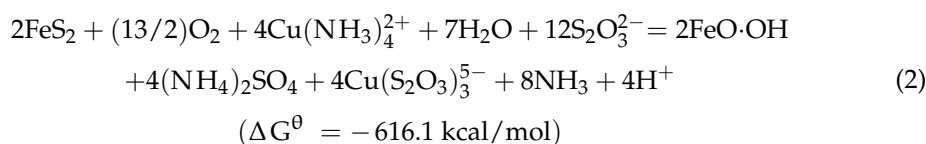
Table 4. The composition and proportion of substances in Figure 9a.

| Binding Energy (eV) | Content (%) | Total Content (%) | Species |
|---------------------|-------------|-------------------|-------------------------|
| 932.93 | 50.0 | 75.0 | Cu ₂ S |
| 952.83 | 25.0 | | |
| 935.02 | 16.7 | 25.0 | CuS/Cu(OH) ₂ |
| 954.92 | 8.3 | | |

Table 5. The composition and proportion of substances in Figure 9b.

| Binding Energy (eV) | Content (%) | Total Content (%) | Species |
|---------------------|-------------|-------------------|---|
| 932.70 | 14.8 | 22.2 | Cu ₂ S |
| 952.60 | 7.42 | | |
| 935.06 | 34.2 | 51.3 | CuS/Cu(OH) ₂ |
| 954.96 | 17.1 | | |
| 940.59 | 7.28 | 26.5 | O ₂ /Cu/Fe interface product |
| 960.49 | 3.64 | | |
| 943.78 | 10.4 | | |
| 963.68 | 5.2 | | |

As shown in Table 3, after 34 h of leaching in the pyrite-only system, many Cu-containing substances were deposited on the gold surface; thus, its Cu content reached 8.48 at%. After fitting, it was found that Cu mainly existed in the form of a CuS passivation layer. The oxidation of pyrite by dissolved oxygen and copper (II) during gold leaching in the Cu²⁺-NH₃-S₂O₃²⁻ system is expressed using the following simplified formula (based on the HSC 6.0 database).



The equilibrium constant logK of the Cu(S₂O₃)₃⁵⁻ complex is greater than that of Cu(en)₂²⁺ (Table 6). Therefore, the Cu⁺ generated via the above formula more easily cooperates with S₂O₃²⁻ to produce Cu(S₂O₃)₃⁵⁻, which resulting in a decrease in the content of Cu(en)₂²⁺, thereby inhibiting the dissolution of gold in the system. In the copper-ethylenediamine-thiosulfate system, Cu(en)₂²⁺ is the substance that can effectively dissolve gold. The free Cu²⁺ in the system reacts with S₂O₃²⁻ and OH⁻ according to Equation (3), resulting in an increased adsorption of CuS on the surface of the gold foil. It can also be known from the literature that pyrite does indeed facilitate the formation of a passivation layer containing copper [7]. Therefore, it can be concluded that the addition of pyrite to the system will impede the dissolution of gold.



When nickel ions and pyrite are added simultaneously, the copper content on the surface of the gold foil is significantly reduced to only 0.5%, primarily existing in the form of Cu₂S. This is because, after the addition of nickel ions and pyrite simultaneously, the Ni(en)₂²⁺ complex is formed by nickel ions in the system and en. Its equilibrium constant of 13.84 is much higher than that of Cu(en)₂²⁺ (10.8), making Ni(en)₂²⁺ easier to form and more stable in the system. The formation of Ni(en)₂²⁺ promotes the reduction of Cu(en)₂²⁺ to Cu(S₂O₃)₃⁵⁻, producing more Cu(S₂O₃)₃⁵⁻. However, with the consumption of S₂O₃²⁻, the Cu⁺, which originally formed Cu(S₂O₃)₃⁵⁻ complex with en is reduced. Therefore, the resulting small quantity of free Cu⁺ combines with the decomposition products of thiosulfate in the system to form Cu₂S (according to Equation (4)). Since the total amount of copper adsorbed on the gold surface in this system is only 0.5%, and the content of

the copper-containing passivation layer is lower, the presence of nickel ions reduces the formation of the copper-containing passivation layer on the gold surface, resulting in faster dissolution of gold compared to when only pyrite is added. Thus, it can be observed that Ni^{2+} effectively weakens the promoting effect of pyrite on the formation of a copper-bearing passivation layer on the gold surface. Therefore, it is concluded that nickel ions and pyrite have a synergistic promoting effect on the dissolution of gold.

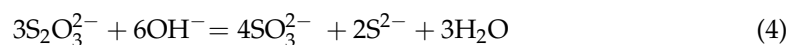


Table 6. The equilibrium constants ($\log K^A$) for the complexation of Ni^{2+} , Cu^+ , Cu^{2+} with en, and $\text{S}_2\text{O}_3^{2-}$: ionic strength ($I = 0$), 25 °C.

| Metal Ion | Complexation | LogK |
|------------------|-----------------------------------|-------|
| Ni^{2+} | Ni(en)^{2+} | 7.52 |
| | Ni(en)_2^{2+} | 13.84 |
| | NiS_2O_3 | 2.06 |
| Cu^+ | Cu(en)_2^+ | 10.8 |
| | $\text{Cu(S}_2\text{O}_3)_3^{5-}$ | 13.84 |
| Cu^{2+} | Cu(en)_2^{2+} | 20 |

A LogK taken from *Lange's Handbook of Chemistry*, 15th ed. [33].

Figure 10a shows the S 2p spectrum corresponding to the surface of gold after leaching in the presence of 1 g of pyrite and Ni^{2+} (8 mg/L). It can be seen from the peak area in Figure 10 that after adding pyrite and Ni^{2+} for leaching, the main sulfur-containing species on the surface of the gold foil is sulfate. The main substance on the surface of the gold foil after leaching only containing pyrite is Cu_2S [32,34]. By comparing Tables 7 and 8, it is found that the Cu_2S content of the sulphide on the surface of the gold foil after leaching in the system containing Ni^{2+} and pyrite is much smaller than that when only pyrite is leached. At the same time, when only pyrite is contained, the surface of the gold foil after leaching is covered with 16.8% of the elemental sulfur [35,36].

Table 7. The composition and proportion of substances in Figure 10a.

| Binding Energy (eV) | Content (%) | Total Content (%) | Species |
|---------------------|-------------|-------------------|---------------------------|
| 161.68 | 12.0 | 18.0 | $\text{CuS/Cu}_2\text{S}$ |
| 162.86 | 6.0 | | |
| 162.86 | 12.5 | 18.8 | FeS_2 |
| 163.87 | 6.25 | | |
| 164.98 | 3.87 | 5.90 | Na_2SO_3 |
| 166.15 | 1.93 | | |
| 168.69 | 38.2 | 57.3 | SO_4^{2-} |
| 169.87 | 19.1 | | |

Table 8. The composition and proportion of substances in Figure 10b.

| Binding Energy (eV) | Content (%) | Total Content (%) | Species |
|---------------------|-------------|-------------------|---------------------------|
| 161.63 | 27.0 | 40.5 | $\text{CuS/Cu}_2\text{S}$ |
| 162.81 | 13.5 | | |
| 163.97 | 11.2 | 16.8 | S |
| 165.15 | 5.60 | | |
| 165.13 | 3.47 | 5.20 | Na_2SO_3 |
| 166.31 | 1.73 | | |
| 168.75 | 25.0 | 37.5 | SO_4^{2-} |
| 169.93 | 12.5 | | |

The above findings and the fact that thiosulphate consumption in the co-presence of pyrite and Ni^{2+} was much greater than that in the presence of pyrite only or Ni^{2+} only suggest that the S-containing substances are mainly produced via thiosulphate decomposition. Moreover, the increase in the amounts of sulfate deposited on the surface of the gold foil leached in the co-presence of Ni^{2+} and pyrite indicate that Ni^{2+} not only hinders the deposition of Cu on the gold surface, but also accelerates the decomposition of thiosulphate to sulphate.

Combined with Figure 11a,b and Tables 9 and 10, it is found that the iron-containing material on the surface of the gold foil after leaching in the system containing Ni^{2+} and pyrite is mainly FeOOH [5,37]. However, the gold surface after leaching in the system containing only pyrite contains a large amount of Fe_2O_3 [38,39], implying that the surface of the gold foil that was leached in the Cu^{2+} -en- $\text{S}_2\text{O}_3^{2-}$ system containing pyrite was covered with $\text{Fe}_2\text{O}_3/\text{Fe}_3\text{O}_4$, possibly due to the oxidation of pyrite and its dissolved Fe species.

Table 9. The composition and proportion of substances in Figure 11a.

| Binding Energy (eV) | Content (%) | Total Content (%) | Species |
|---------------------|-------------|-------------------|--|
| 706.91 | 2.6 | 3.9 | FeS ₂ |
| 720.51 | 1.3 | | |
| 710.50 | 7.07 | 10.6 | Fe ₂ O ₃ /Fe ₃ O ₄ |
| 724.10 | 3.53 | | |
| 711.90 | 35.6 | 53.4 | FeOOH |
| 725.50 | 17.8 | | |
| 720.03 | 21.4 | 32.1 | O ₂ /Cu/Fe interface product |
| 733.63 | 10.7 | | |

Table 10. The composition and proportion of substances in Figure 11b.

| Binding Energy (eV) | Content (%) | Total Content (%) | Species |
|---------------------|-------------|-------------------|--|
| 706.94 | 3.44 | 5.16 | FeS ₂ |
| 720.54 | 1.69 | | |
| 710.87 | 49.0 | 73.5 | Fe ₂ O ₃ /Fe ₃ O ₄ |
| 724.47 | 24.5 | | |
| 717.60 | 10.7 | 16.1 | O ₂ /Cu/Fe interface product |
| 731.20 | 5.40 | | |
| 719.92 | 3.49 | 5.24 | product |
| 733.52 | 1.75 | | |

Based on the above findings, the following conclusions were drawn. In the system containing only pyrite, the passivation film on the gold surface is mainly composed of Cu_2S , S_0 , Fe_2O_3 , etc. In the presence of both pyrite and Ni^{2+} , the Cu species on the gold surface were no longer dominant and were largely replaced by Fe- and S-containing compounds, indicating that Ni^{2+} alleviated the deposition of Cu-containing materials on the surface of the gold foil. This greatly hindered the passivation of the gold foil and facilitated its contact with the leaching fluid to accelerate gold dissolution.

3.5.2. XPS Analysis of the Pyrite Surface after Leaching

Tables 11 and 12 show the elemental composition of the pyrite surface after leaching in the presence of both Ni^{2+} and pyrite and pyrite only, respectively. Compared with the elemental composition of the pyrite surface obtained in the pyrite-only case, that obtained in the presence of both Ni^{2+} and pyrite contained small amounts of Au and Cu as well as surface-adsorbed Ni.

Table 11. Atomic concentration of pyrite (1 g) leached in the Cu^{2+} -en- $\text{S}_2\text{O}_3^{2-}$ system in the presence Ni^{2+} (8 mg/L).

| Element | O | S | Fe | Ni | Cu | Au |
|-------------------|------|------|------|------|------|------|
| Concentration (%) | 77.0 | 13.4 | 7.70 | 0.26 | 1.50 | 0.14 |

Table 12. Atomic concentration of pyrite (1 g) leached in the Cu^{2+} -en- $\text{S}_2\text{O}_3^{2-}$ system without Ni^{2+} .

| Element | O | S | Fe | Cu | Au |
|-------------------|------|------|------|----|----|
| Concentration (%) | 60.4 | 27.8 | 11.8 | 0 | 0 |

Figure 12a,b show the fitted Fe 2p spectra of pyrite recorded after leaching in the presence of 1 g of pyrite and Ni^{2+} (8 mg/L) and 1 g of pyrite only, respectively. The iron-containing substance on the pyrite surface after leaching in the presence of Ni^{2+} is FeOOH [12,40]. The surface of the pyrite leached in the Ni-free system showed mainly FeS_2 and $\text{Fe}_2\text{O}_3/\text{Fe}_3\text{O}_4$ (as show Tables 13 and 14). Obviously, when Ni^{2+} and pyrite were present in the leaching system, FeOOH was formed on the surface of the leached pyrite. According to the literature, at pH values in the range 9–10, the oxidation potential of pyrite is as low as -0.4 to -0.3 V [8], and during gold leaching in the ammonia–thiosulphate system, pyrite can be oxidised to FeOOH by dissolved O_2 and Cu (II) (according to Equation (2)).

Table 13. The composition and proportion of substances in Figure 12a.

| Binding Energy (eV) | Content (%) | Total Content (%) | Species |
|---------------------|-------------|-------------------|----------------|
| 706.51 | 4.26 | 6.4 | FeS_2 |
| 720.11 | 2.14 | | |
| 711.50 | 62.4 | 93.6 | FeOOH |
| 725.10 | 31.2 | | |

Table 14. The composition and proportion of substances in Figure 12b.

| Binding Energy (eV) | Content (%) | Total Content (%) | Species |
|---------------------|-------------|-------------------|--|
| 706.36 | 17.6 | 26.4 | FeS_2 |
| 719.96 | 8.8 | | |
| 710.87 | 28.4 | 42.6 | Fe_3O_4 |
| 724.47 | 14.2 | | |
| 711.80 | 14.3 | 21.45 | FeOOH |
| 725.40 | 7.15 | | |
| 719.56 | 5.19 | 7.79 | $\text{O}_2/\text{Cu}/\text{Fe}$ interface product |
| 733.16 | 2.60 | | |
| 721.93 | 1.17 | 1.76 | |
| 735.53 | 0.59 | | |

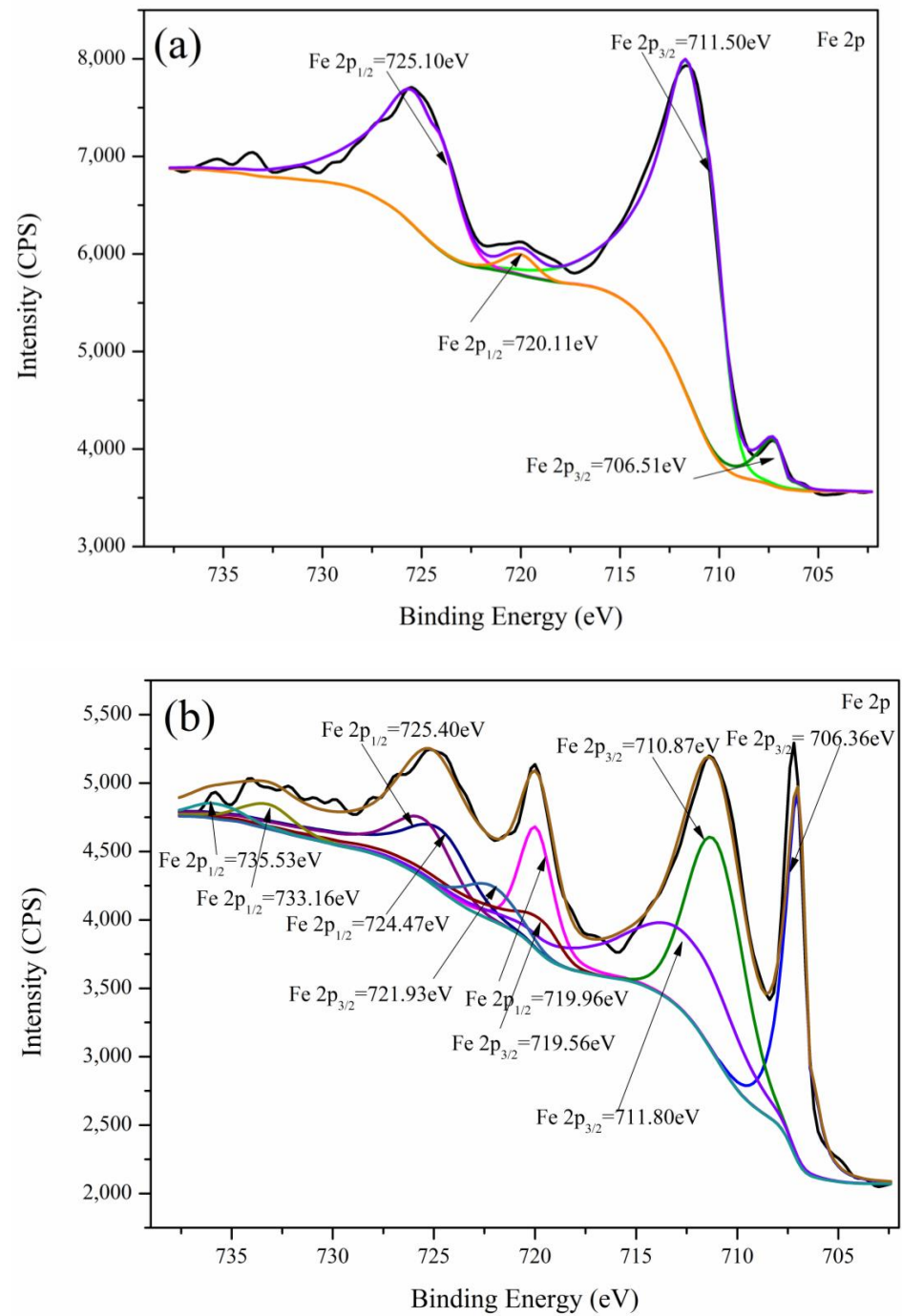


Figure 12. Fe 2p XPS spectra corresponding to pyrite surfaces after leaching in the presence of pyrite (1 g). (a) With the addition of Ni²⁺ and (b) without the addition of Ni²⁺.

3.6. Tafel Curves

The electrokinetic polarisation of gold foil was studied in different systems within a scan range of -0.5 – 0 V and at a scan rate of 1 mV/s. The thus-obtained Tafel curves (Figure 13) were used to determine the Au corrosion potential (E_{corr}) as well as corrosion current density (j_{corr}) (Table 15).

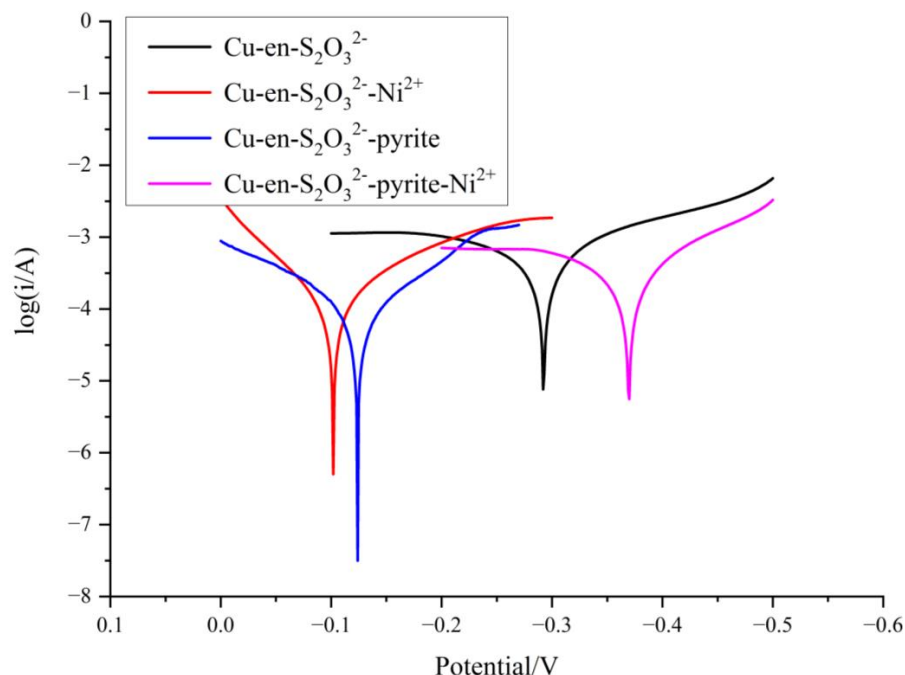


Figure 13. Tafel curves corresponding to gold foil in different solution systems, at a scan rate of 1 mV/s (potential scan rate, 2 mV/s; rotation speed, 300 rpm).

Table 15. Tafel parameters corresponding to gold foil in different solution systems.

| System | E_{corr} (V) | J_{corr} (A) |
|---|-----------------------|-----------------------|
| $\text{Cu}^{2+}\text{-en-S}_2\text{O}_3^{2-}$ | -0.29 | 1.27×10^{-3} |
| $\text{Cu}^{2+}\text{-en-S}_2\text{O}_3^{2-}\text{-Ni}^{2+}$ | -0.08 | 4.03×10^{-4} |
| $\text{Cu}^{2+}\text{-en-S}_2\text{O}_3^{2-}\text{-pyrite}$ | -0.12 | 4.14×10^{-4} |
| $\text{Cu}^{2+}\text{-en-S}_2\text{O}_3^{2-}\text{-pyrite-Ni}^{2+}$ | -0.37 | 1.03×10^{-3} |

In the $\text{Cu}^{2+}\text{-en-S}_2\text{O}_3^{2-}$ system, a 1.5 cm \times 1.5 cm piece of gold foil was used as the working electrode, and for blank controls, E_{corr} and j_{corr} were determined as -0.29 V and 1.27×10^{-3} A, respectively. In the presence of Ni^{2+} (8 mg/L) only, E_{corr} increased to -0.08 V, while j_{corr} decreased to 4.03×10^{-4} A, indicating a weakening of the corrosion of the gold foil surface. Furthermore, in the presence of pyrite only, the Fe-containing substances resulting from pyrite oxidation formed a precipitate and attached to the electrode surface, further hindering the oxidation of Au. Therefore, compared with the blank $\text{Cu}^{2+}\text{-en-S}_2\text{O}_3^{2-}$ system, the electrode corrosion potential increased, while the current density decreased. When both Ni^{2+} (8 mg/L) and pyrite were added to the leaching system, E_{corr} decreased, indicating that the gold foil became more prone to corrosion. This finding is consistent with the results of the leaching experiments, indicating that the synergistic effect of Ni^{2+} and pyrite on gold dissolution could be ascribed to the decrease in E_{corr} and the increase of j_{corr} . Considering the results of XPS analysis obtained for leached gold foil as well, it became evident that the addition of both Ni^{2+} and pyrite significantly hindered the adhesion of Cu_2S or CuS on the gold surface, and under these conditions, the main compound that was deposited on the Au foil surface during leaching was identified as FeOOH . Furthermore, SEM imaging revealed that these precipitates that were deposited on the gold foil surface after leaching were loose and amorphous; hence, their inhibitory effect on gold foil corrosion was limited.

4. Conclusions

In this paper, the effects of nickel ions and pyrite on the amount of reagent and the amount of gold extraction in a copper-thylenediamine-thiosulfate leaching system were studied. The synergistic effect of nickel ions and pyrite on gold dissolution in a Cu^{2+} -en- $\text{S}_2\text{O}_3^{2-}$ leaching system was discussed in detail, and the related mechanism was studied. The following conclusions were drawn:

1. The addition of Ni^{2+} or pyrite to the Cu^{2+} -en- $\text{S}_2\text{O}_3^{2-}$ gold-leaching system could significantly inhibit the dissolution of gold and promote the decomposition of thiosulfate.
2. When both pyrite and Ni^{2+} were simultaneously present in the leaching system, they synergistically promoted gold dissolution. The synergistic action of these two substances could increase the concentration of gold to $22.5 \text{ mg/L}\cdot\text{cm}^2$.
3. In the pyrite-only Cu^{2+} -en- $\text{S}_2\text{O}_3^{2-}$ gold-leaching system, the surface of the gold foil was found to contain a large amount of copper-containing sulphide layers after leaching. However, hardly any Cu was detected on the surface of the gold foil that was leached in the co-presence of pyrite and Ni^{2+} . Thus, Ni^{2+} ions effectively weakened the promotional effect of pyrite on the formation of the Cu-containing passivation layer on the gold surface.
4. Tafel polarisation curves showed that the addition of Ni^{2+} or pyrite only increased the corrosion potential of Au; thus, gold dissolution was inhibited. However, in the presence of both Ni^{2+} and pyrite, the corrosion potential of Au decreased, resulting in an acceleration of the amount of gold dissolution.

Supplementary Materials: The following supporting information can be downloaded at: <https://www.mdpi.com/article/10.3390/min14010002/s1>.

Author Contributions: X.Q. Writing—original draft; Writing—review & editing; T.Z. Funding acquisition; F.Z.: Conceptualization; Resources: H.Z.: Supervision; G.L.: Investigation. All authors have read and agreed to the published version of the manuscript.

Funding: This research was funded by [Natural Science Foundation of China] grant number [51674128], [Inner Mongolia University of Technology] grant number [ZZ202115] and [Inner Mongolia Autonomous Region Department of Education] grant number [JY20220155].

Data Availability Statement: Data are contained within the article.

Conflicts of Interest: The authors declare no conflict of interest.

References

1. Wang, J.; Lu, Y.; Xu, Z. Identifying Extraction Technology of Gold from Solid Waste in Terms of Environmental Friendliness. *ACS Sustain. Chem. Eng.* **2019**, *7*, 7260–7267. [[CrossRef](#)]
2. Aylmore, M.G.; Muir, D.M. Thiosulfate leaching of gold—A review. *Miner. Eng.* **2001**, *14*, 135–174. [[CrossRef](#)]
3. Xu, B.; Kong, W.; Li, Q.; Yang, Y.; Jiang, T.; Liu, X. A Review of Thiosulfate Leaching of Gold: Focus on Thiosulfate Consumption and Gold Recovery from Pregnant Solution. *Metals* **2017**, *7*, 222. [[CrossRef](#)]
4. Kakumazaki, J.; Kato, T.; Sugawara, K. Recovery of Gold from Incinerated Sewage Sludge Ash by Chlorination. *ACS Sustain. Chem. Eng.* **2014**, *2*, 2297–2300. [[CrossRef](#)]
5. Xu, B.; Yang, Y.; Li, Q.; Jiang, T.; Zhang, X.; Li, G. Effect of common associated sulfide minerals on thiosulfate leaching of gold and the role of humic acid additive. *Hydrometallurgy* **2017**, *171*, 44–52. [[CrossRef](#)]
6. Tao, J.; Shi, X.; Jin, C.; Tang, Y. Anodic oxidation of thiosulfate ions in gold leaching. *J. Cent. South Univ. Technol.* **1997**, *4*, 89–91.
7. Feng, D.; van Deventer, J.S.J. Ammoniacal thiosulphate leaching of gold in the presence of pyrite. *Hydrometallurgy* **2006**, *82*, 126–132. [[CrossRef](#)]
8. Liu, X.; Xu, B.; Min, X.; Li, Q.; Yang, Y.; Jiang, T.; He, Y.; Zhang, X. Effect of Pyrite on Thiosulfate Leaching of Gold and the Role of Ammonium Alcohol Polyvinyl Phosphate (AAPP). *Metals* **2017**, *7*, 278. [[CrossRef](#)]
9. Melashvili, M.; Fleming, C.; Dymov, I.; Matthews, D.; Dreisinger, D. Dissolution of gold during pyrite oxidation reaction. *Miner. Eng.* **2016**, *87*, 2–9. [[CrossRef](#)]
10. Feng, D.; van Deventer, J.S.J. The effect of sulphur species on thiosulphate leaching of gold. *Miner. Eng.* **2007**, *20*, 273–281. [[CrossRef](#)]

11. Senanayake, G.; Zhang, X.M. Gold leaching by copper(II) in ammoniacal thiosulphate solutions in the presence of additives. Part II: Effect of residual Cu(II), pH and redox potentials on reactivity of colloidal gold. *Hydrometallurgy* **2012**, *115–116*, 21–29. [[CrossRef](#)]
12. Feng, D.; Deventer, J.S.J.V. The role of heavy metal ions in gold dissolution in the ammoniacal thiosulphate system. *Hydrometallurgy* **2002**, *64*, 231–246. [[CrossRef](#)]
13. Fotoohi, B.; Mercier, L. Recovery of precious metals from ammoniacal thiosulfate solutions by hybrid mesoporous silica: 1-Factors affecting gold adsorption. *Sep. Purif. Technol.* **2014**, *127*, 84–96. [[CrossRef](#)]
14. Dangi, Y.R.; Lin, X.Y.; Choi, J.W.; Lim, C.R.; Song, M.H.; Han, M.; Bediako, J.K.; Cho, C.W.; Yun, Y.S. Polyethyleneimine functionalized alginate composite fiber for fast recovery of gold from acidic aqueous solutions. *Environ. Technol. Innov.* **2022**, *28*, 102605. [[CrossRef](#)]
15. Arima, H.; Fujita, T.; Yen, W.T. Using Nickel as a Catalyst in Ammonium Thiosulfate Leaching for Gold Extraction. *Mater. Trans.* **2004**, *45*, 516–526. [[CrossRef](#)]
16. Xu, B.; Li, K.; Li, Q.; Yang, Y.; Liu, X.; Jiang, T. Kinetic studies of gold leaching from a gold concentrate calcine by thiosulfate with cobalt-ammonia catalysis and gold recovery by resin adsorption from its pregnant solution. *Sep. Purif. Technol.* **2019**, *213*, 368–377. [[CrossRef](#)]
17. Wang, Q.; Hu, X.; Zi, F.; Yang, P.; Chen, Y.; Chen, S. Environmentally friendly extraction of gold from refractory concentrate using a copper—Ethylenediamine—Thiosulfate solution. *J. Clean. Prod.* **2019**, *214*, 860–872. [[CrossRef](#)]
18. Chen, S.; Zi, F.; Hu, X.; Chen, Y.; Yang, P.; Wang, Q.; Qin, X.; Cheng, H.; Liu, Y.; He, Y.; et al. Interfacial properties of mercaptopropyl-functionalised silica gel and its adsorption performance in the recovery of gold(I) thiosulfate complex. *Chem. Eng. J.* **2020**, *393*, 124547. [[CrossRef](#)]
19. Yang, Y.-B.; Zhang, X.; Xu, B.; Li, Q.; Jiang, T.; Wang, Y.-X. Effect of arsenopyrite on thiosulfate leaching of gold—ScienceDirect. *Trans. Nonferrous Met. Soc. China* **2015**, *25*, 3454–3460. [[CrossRef](#)]
20. Dang, X.-E.; Ke, W.-S.; Tang, C.; Lv, J.; Zhou, X.; Liu, C.-P. Increasing leaching rate of gold cyanide of two-stage calcination generated from refractory ore containing arsenopyrite and pyrrhotite. *Rare Met.* **2015**, *35*, 804–810. [[CrossRef](#)]
21. Feng, D.; van Deventer, J.S.J. Effect of hematite on thiosulphate leaching of gold. *Int. J. Miner. Process.* **2007**, *82*, 138–147. [[CrossRef](#)]
22. Feng, D.; van Deventer, J.S.J. Effect of Sulfides on Gold Dissolution in Ammoniacal Thiosulfate Medium. *Metall. Mater. Trans. B* **2005**, *34B*, 5–13. [[CrossRef](#)]
23. Xu, Y.; Schoonen, M.A. The stability of thiosulfate in the presence of pyrite in low-temperature aqueous solutions. *Geochim. Cosmochim. Acta* **1995**, *59*, 4605–4622. [[CrossRef](#)]
24. Schippers, A.; Sand, W. Bacterial leaching of metal sulfides proceeds by two indirect mechanisms via thiosulfate or via polysulfides and sulfur. *Appl. Environ. Microbiol.* **1999**, *65*, 319–321. [[CrossRef](#)] [[PubMed](#)]
25. Byerley, J.; Fouda, S.; Rempel, G. Kinetics and mechanism of the oxidation of thiosulphate ions by copper(II) ions in aqueous ammonia solution. *J. Chem. Soc.-Dalton Trans.* **1973**, *8*, 889–893. [[CrossRef](#)]
26. Chu, C.K.; Breuer, P.L.; Jeffrey, M.I. The impact of thiosulfate oxidation products on the oxidation of gold in ammonia thiosulfate solutions. *Miner. Eng.* **2003**, *16*, 265–271. [[CrossRef](#)]
27. Bagdasaryan, K.A.; Episkoposyan, M.L.; Ter-Arakelyan, K.A.; Babayan, G.G. Study of the Dissolution Kinetics of Gold and Silver in Sodium Thiosulfate Solutions, *Izvestiya Vysshikh Uchebnykh Zavedenij. Tsvetnaya Metall.* **1983**, *5*, 64–68.
28. Pedraza, A.M.; Villegas, I.; Freund, P.L.; Chornik, B. Electro-oxidation of thiosulphate ion on gold: Study by means of cyclic voltammetry and auger electron spectroscopy. *J. Electroanal. Chem. Interfacial Electrochem.* **1988**, *250*, 443–449. [[CrossRef](#)]
29. Sun, X.; Guan, Y.C.; Han, K.N. Electrochemical Behavior of the Dissolution of Gold-Silver Alloys in Cyanide Solutions. *Metall. Mater. Trans. B* **1996**, *27B*, 355–361. [[CrossRef](#)]
30. Perry, D.L.; Taylor, J.A. X-ray photoelectron and Auger spectroscopic studies of Cu₂S and CuS. *J. Mater. Sci. Lett.* **1986**, *5*, 384–386. [[CrossRef](#)]
31. Deroubaix, G.; Marcus, P. X-ray Photoelectron Spectroscopy Analysis of Copper and Zinc Oxides and Sulphides. *Surf. Interface Anal.* **1992**, *18*, 39–46. [[CrossRef](#)]
32. Acres, R.G.; Harmer, S.L.; Beattie, D.A. Synchrotron XPS studies of solution exposed chalcopyrite, bornite, and heterogeneous chalcopyrite with bornite. *Int. J. Miner. Process.* **2010**, *94*, 43–51. [[CrossRef](#)]
33. Dean, J.A. *Lange's Handbook of Chemistry*, 15th ed.; McGraw-Hill: New York, NY, USA, 1998.
34. Velásquez, P.; Leinen, D.; Pascual, J.; Ramos-Barrado, J.R.; Córdova, R. A chemical; morphological; electrochemical (XPS, SEM/EDX, and EIS) analysis of electrochemically modified electrode surfaces of natural chalcopyrite (CuFeS₂) and pyrite (FeS₂) in alkaline solutions. *J. Phys. Chem. B* **2005**, *109*, 4977–4988. [[CrossRef](#)] [[PubMed](#)]
35. Goh, S.W.; Buckley, A.N.; Lamb, R.N.; Rosenberg, R.A.; Moran, D. The oxidation states of copper and iron in mineral sulfides, and the oxides formed on initial exposure of chalcopyrite and bornite to air. *Geochim. Cosmochim. Acta* **2006**, *70*, 2210–2228. [[CrossRef](#)]
36. Laajalehto, K.; Kartio, I.; Nowak, P. XPS study of clean metal sulfide surfaces. *Appl. Surf. Sci.* **1994**, *81*, 11–15. [[CrossRef](#)]
37. Nava, D.; González, I.; Leinen, D.; Ramos-Barrado, J.R. Surface characterization by X-ray photoelectron spectroscopy and cyclic voltammetry of products formed during the potentiostatic reduction of chalcopyrite. *Electrochim. Acta* **2008**, *53*, 4889–4899. [[CrossRef](#)]
38. Daas, H.D.; Passacantando, M.; Lozzi, L.; Santucci, S.; Picozzi, P. The interaction of Cu(100)-Fe surfaces with oxygen studied by X-ray photoelectron spectroscopy. *Surf. Sci.* **1994**, *317*, 295–302. [[CrossRef](#)]

39. Oscarson, D.W.; Huang, P.M. Oxidative power of Mn (IV) and Fe (III) oxides with respect to As (III) in terrestrial and aquatic environments. *Nature* **1981**, *291*, 50–51. [[CrossRef](#)]
40. Xu, B.; Li, K.; Dong, Z.; Yang, Y.; Li, Q.; Liu, X.; Jiang, T. Eco-friendly and economical gold extraction by nickel catalyzed ammoniacal thiosulfate leaching-resin adsorption recovery. *J. Clean. Prod.* **2019**, *233*, 1475–1485. [[CrossRef](#)]

Disclaimer/Publisher’s Note: The statements, opinions and data contained in all publications are solely those of the individual author(s) and contributor(s) and not of MDPI and/or the editor(s). MDPI and/or the editor(s) disclaim responsibility for any injury to people or property resulting from any ideas, methods, instructions or products referred to in the content.